OPEN

Correspondence and
requests for materials
should be addressed to
S.H.R. (reedsh1@
cardiff.ac.uk)

3D-DIP-Chip: a microarray-based method to measure genomic DNA damage

James Rees Powell[1], Mark Richard Bennett[1], Katie Ellen Evans[1], Shirong Yu[1], Richard Michael Webster[1], Raymond Waters[1], Nigel Skinner[2] & Simon Huw Reed[1]

[1]Cancer & Genetics Building, Cardiff University, School of Medicine, Heath Park, Cardiff, CF14 4XN, UK, [2]Agilent Technologies (UK) Ltd, 710 Wharfedale Road, Winnersh Triangle, Wokingham, Berkshire, RG41 5TP, UK.

Genotoxins cause DNA damage, which can result in genomic instability. The genetic changes induced have far-reaching consequences, often leading to diseases such as cancer. A wide range of genotoxins exists, including radiations and chemicals found naturally in the environment, and in man-made forms created by human activity across a variety of industries. Genomic technologies offer the possibility of unravelling the mechanisms of genotoxicity, including the repair of genetic damage, enhancing our ability to develop, test and safely use existing and novel materials. We have developed 3D-DIP-Chip, a microarray-based method to measure the prevalence of genomic genotoxin-induced DNA damage. We demonstrate the measurement of both physical and chemical induced DNA damage spectra, integrating the analysis of these with the associated changes in histone acetylation induced in the epigenome. We discuss the application of the method in the context of basic and translational sciences.

The DNA molecule is highly susceptible to damage from a variety of genotoxins, both natural and man-made. Endogenous DNA damage occurs spontaneously, at high rates, as a consequence of normal cellular processes including oxidative reactions, resulting in DNA base modifications, and a variety of errors introduced during DNA replication. Exogenous DNA damage occurs due to chemical or physical insults, including radiations present in the environment and man-made chemicals. These often induce the formation of bulky adducts, cross-links and strand breaks in the DNA, which if not repaired correctly can lead to cell death or the proliferation of mutations. To ensure cell survival and to maintain the integrity of the genome, sophisticated networks of DNA repair pathways have evolved. These are critical to maintaining health and preventing genetic mutations, which may result in disease development and drive carcinogenesis.

Mutations induced in DNA by genotoxic agents are a product of DNA damage caused by exposure of cells to those agents, and the cells' capacity to subsequently repair that damage. The ability to sensitively measure genome-wide levels and locations of genetic damage, and rates of its removal by DNA repair, has major significance in a range of applications. In addition to determining the mechanisms of DNA damage induction and DNA repair processes in basic research, such a method may be employed in a variety of other settings. For example, current genotoxicity testing uses overly simplistic assays, often relying on animal models[1]. Novel *in vitro* methods are being developed and a microarray-based tool for measuring DNA damage and repair would represent a significant advance in this area. Similarly, clinicians using DNA damaging chemotherapeutic drugs — mainstays in the treatment of patients with solid tumours — would benefit enormously from a method capable of predicting response to these agents based on the detection of genomic DNA damage and repair signatures. The development of such a method would represent an important advance and would enable personalisation of therapies. Recent advances in DNA sequencing technologies now permit whole genome mutation analyses, and the sequencing of individual cancer genomes has revealed the presence of mutational signatures within the genomes of cancer cells[2]. The ability to detect and measure DNA damage and repair spectra with a view to associating these with the mutational end-points detected in cancer genomes would enable these early indicators to be used as predictive markers for the subsequent mutational endpoints. These may include markers which predict predisposition to, and the progression of, disease, as well as the ability to determine the response of individuals to drug treatments of these diseases.

Here we present and, importantly, validate a novel, patented method to measure the locations and levels of genotoxin-induced DNA damage throughout genomes, or sections thereof, named 3D-DIP-chip: DNA Damage Detection (3D) by DNA Immuno-Precipitation (DIP) on microarray chips (Chip). We describe for the first time the definitive protocols for the use of this method in both yeast and human cells. This method enables the examination and mapping of DNA damage at a high resolution throughout any sequenced genome (Figure 1). We demonstrate the technology with DNA damage induced by three genotoxins: a natural physical source (UV radiation) and two synthetic chemical sources (the platinating chemotherapeutic drugs cisplatin and oxaliplatin) in cultured human cells and in *Saccharomyces cerevisiae*.

We also demonstrate how these 3D-DIP-Chip datasets may be examined in association with additional ChIP-chip datasets to carry out integrated analyses of a variety of different data. In the work presented here we investigate histone H3 lysine 14 (H3K14) acetylation changes in response to these DNA damaging agents using ChIP-chip in *S. cerevisiae*. Epigenetic changes in histone H3 acetylation are known to be an important cellular response to DNA damage, controlling the chromatin structure in the nuclei of cells, promoting efficient DNA repair[3,4]. We compare these epigenetic changes induced by UV and platinum DNA adduct formation in cells in the context of the respective DNA damage spectra. We demonstrate how the integrated analysis of these related datasets, which is made

possible via the bioinformatic software package Sandcastle developed in our laboratory, reveals the potential for gaining a systems view of genome stability, revealing how organisms organise and orchestrate their responses to genetic damage.

Results

Workflow. The 3D-DIP-Chip experimental workflow is described in detail in the Methods section of this report. The procedure is outlined in Figure 1. Briefly, protein cross-linked chromatin or damaged DNA is extracted from cells and fragmented by sonication (Figure 1a, top and bottom respectively). Fragments of interest are affinity captured by immunoprecipitation (IP) using an antibody raised against that feature of interest, for example a damage induced DNA adduct, a DNA binding protein or a post-translationally modified histone (Figure 1b). Initial input (IN) samples are also collected. Following IP, DNA damages or DNA-protein cross-links are reversed, DNA is purified and IP and IN samples are amplified, differentially labelled using a two-dye system and applied to DNA microarrays covering the genome of interest (Figure 1c). After hybridisation the microarrays are washed and optically scanned (Figure 1d), and the fluorescence intensity values recorded for each probe representing a location of the genome are converted to numerical values, which can be analysed and plotted (Figure 1e). The data from these files are loaded into the R statistical programming environment (R Development Core Team. *R: A language and environment for statistical computing. R foundation for statistical computing* (Vienna, Austria, 2011)) for analysis, and analysed using Sandcastle, a suite of tools for the normalisation, analysis and graphical display of ChIP-chip data. The Sandcastle software and full documentation are available for download from http://reedlab.cardiff.ac.uk/sandcastle

Affinity capturing damaged DNA. Monoclonal antibodies for UV-induced CPDs and platinum-induced guanine adducts were used to affinity capture DNA damaged with the respective agents, with the resulting enrichment assessed by Q-PCR (full details are given in the Methods section). Dose-dependent enrichment is demonstrated for DNA from both yeast and human cells treated with cisplatin and oxaliplatin (Supplementary Fig. S1 a and b respectively), confirming the known characteristic that oxaliplatin forms fewer adducts than cisplatin at equimolar doses[5–7]. This demonstrates that 3D-DIP is a reliable method of affinity capturing DNA damaged by different genotoxins.

Removing DNA damage lesions prior to PCR amplification. The IN and 3D-DIP samples contain DNA damage. Many DNA adducts, including CPDs and platinum adducts, inhibit DNA polymerases[8,9] which can restrict efficient downstream processing of samples by PCR. Removal of the damage is therefore required to carry out the full 3D-DIP-Chip procedure. Platinum-DNA adducts are very stable over a long period of time, but in the presence of cyanide ions most platinum residues are known to be removed from DNA[10]. Sodium cyanide (NaCN) has been proven to be the most effective chemical for disrupting platinum-DNA adducts[10–12], and in the DIP studies described in this paper, NaCN was used to remove platinum adducts. Similarly, CPDs also need removal prior to downstream processing and this was achieved using a PreCR DNA repair kit (See Methods for details). Supplementary Fig. S2a demonstrates the effectiveness of NaCN in removing adducts from cisplatin and oxaliplatin treated human DNA. Platinum damaged DNA treated with NaCN prior to immunoprecipitation shows no enrichment following immunoprecipitation, demonstrating removal of the platinum adducts. Effective DNA damage removal following immunoprecipitation of platinum induced adducts was also confirmed by demonstrating greater qRT-PCR amplification in DNA samples processed for damage removal after immunoprecipitation (Supplementary Fig. S2 b and c).
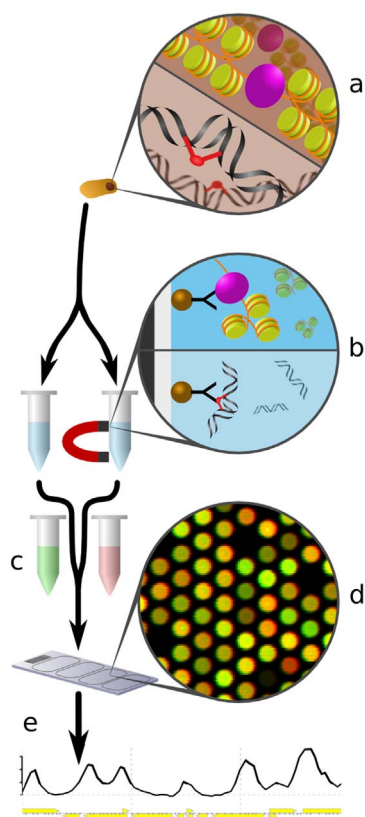

Figure 1 | Representation of the 3D-DIP-Chip and ChIP-Chip procedure. (a) Proteins are crosslinked to chromatin (top) or DNA damage is induced (bottom). This DNA or chromatin is extracted, sonicated and split into two samples. (b) IP is carried out on one sample to separate the chromatin bound factor of interest (top) or damaged DNA (bottom). (c) Both samples are purified, amplified by PCR and differentially labelled with red or green fluorophores. (d) The samples are allowed to hybridise to the microarray probes and the resulting intensity values from the scanned image are converted to numerical values. (e) These values may be plotted and processed as required by the investigation.

Measuring DNA damage on DNA microarrays. To determine the levels and locations of DNA damage, the human and yeast derived samples were hybridised to two-colour Agilent 4x44K microarrays. Human samples were analysed on a custom-designed microarray covering a randomly selected section of the genome: 10 Mbp of chromosome 17. Yeast samples were analysed with the G4493A whole genome microarray. Log$_2$ IP:IN ratio values are used for all analyses giving relative levels of DNA adducts detected at the genomic locations represented by the probes on the microarray. Data from files created by Agilent's Feature Extraction Software (version 10.10) were loaded into R for analysis. Reproducibility was assessed by calculating Spearman's rank correlation coefficients between datasets (Table 1), demonstrating the range of correlation values for the respective categories described. The average of two human *in vitro* cisplatin treated datasets is shown as a Circos plot in Fig. 2a, demonstrating the heterogeneity of the DNA damage distribution over the 10 Mbp genome section analysed. A 25 Kbp section of the data is shown in more detail in Fig. 2b, showing the mean and standard error of the mean of the two datasets. Overall reproducibility is also shown as a scatter plot of one dataset against the other for the total cisplatin (Fig. 2c) and oxaliplatin (Fig. 2d) data, with corresponding Spearman's rank correlation coefficient values shown in Table 1. Similar figures for oxaliplatin and UV-induced CPD damage datasets are shown in Supplementary Figure S3 a and b, c and d respectively.

Validating DNA damage profiles. Employing predicted DNA damage profiles, against which the actual damage datasets are compared, can validate the accuracy of the 3D-DIP-chip technology. This process has been applied previously[13]. Cisplatin and oxaliplatin have been shown previously to induce DNA damage at purine bases, forming 1,2-d(GpG), 1,2-d(ApG), 1,3-d(Gp-NpG) intrastrand crosslinks, and interstrand guanine crosslinks in the ratio $65:25:7:3$[6,14,15]. Similarly, UV irradiation has been shown previously to induce damage at dipyrimidine sites, forming CPDs at TT, TC, CT, and CC sites in the ratio $68:16:13:3$[16,17]. These ratios were used in conjunction with the genome sequence to predict the level of expected damage for each probe on the microarray. Spearman's rank correlation coefficient values were calculated for each microarray dataset versus the predicted pattern for comparison (Table 1). A 25Kbp section of the human *in vitro* treated cisplatin dataset and predicted profile is also shown in Fig. 3, demonstrating the level of concordance between the two. The variability seen around position 10,320,000 is caused by the lack of features printed on the array over this region. This is demonstrated by the absence of grey dots that indicate the genomic position of these features at the bottom of the figure.

Bioinformatic analysis of genetic and epigenetic genome-wide datasets. We have shown genomic DNA damage profiles for two different forms of DNA damage in human DNA. Genetic damage also induces epigenetic changes in the form of histone modifications[4]. To investigate how these two parameters relate to each other in response to genotoxic exposure we treated yeast cells with the same genotoxins. Genome plots for UV and cisplatin damaged DNA are presented in Supplementary Fig. S4. Alongside this we employed ChIP-chip to measure the DNA damage induced changes in histone H3 acetylation at lysine 9, which is known to be required for the efficient repair of UV-induced CPDs. To do this we measured the background histone H3 acetylation levels before inducing DNA damage and repeated these measurements after DNA damage, in order to determine the DNA damage induced change. Figure 4 demonstrates the results of measuring the distribution of genetic damage induced in the genome by exposing yeast cells either to UV light or to treatment with cisplatin. Different DNA damage profiles are generated from these different damaging agents as demonstrated by the negative Spearman's rank correlation (Figure 4a. See also Supplementary Fig. S4), which reflects the fact that different DNA damaging agents induce damage at different dipyrimidine and dipurine bases. Indeed, by analysing and plotting the same data in relation to transcriptional start sites located throughout the genome (Figure 4b) it is possible to visualise the different patterns of cisplatin damage (solid black line) versus UV induced damage (solid green line). By plotting the predicted damage spectra for both cisplatin (dashed black line) and UV (dashed green line) induced DNA damage, as expected, it can be seen that the actual damage profile generally follows the predicted pattern. Significantly however, regions where these patterns deviate from the prediction can be observed, particularly in the promoter regions of genes upstream of the transcriptional start site, but also at specific locations in the open reading frames. This is particularly evident in the case of cisplatin damage where lower levels of damage are observed in the promoter regions of genes than might be expected based on the predicted pattern (see Discussion). This result demonstrates the significance of this technique as a tool for analysing DNA damage throughout genomes. Analysis of the spectrum of DNA damage-induced histone acetylation reveals a positive association between the UV versus the cisplatin induced DNA damage treatments (Figure 4c). As expected, this is confirmed when plotting the same data in relation to all genomic transcription start sites (Figure 4d). However, plotting the data in this context reveals the genomic location of a peak of DNA damage induced histone H3 acetylation that is observed immediately downstream of the transcription start site, just inside the open reading frame. These results indicate that the DNA damage-induced increase in histone H3 acetylation, which is known to be important for the response to and repair of DNA damage in chromatin, appears to be very similar, regardless of the individual patterns of DNA damage induced, or whether a physical or chemical DNA damaging agent is used. This may reflect DNA damage-induced changes in the epigenome and chromatin structure that

Table 1 | Spearman's rank correlation ρ values for 3D-DIP-Chip data of physically and chemically induced DNA damage in human and yeast samples treated *in vivo* and *in vitro*. Correlations with prediction are calculated from the predicted profiles created in Sandcastle. Correlations between replicates are calculated from two individual microarray datasets. UV induced DNA damage in yeast was not investigated here.

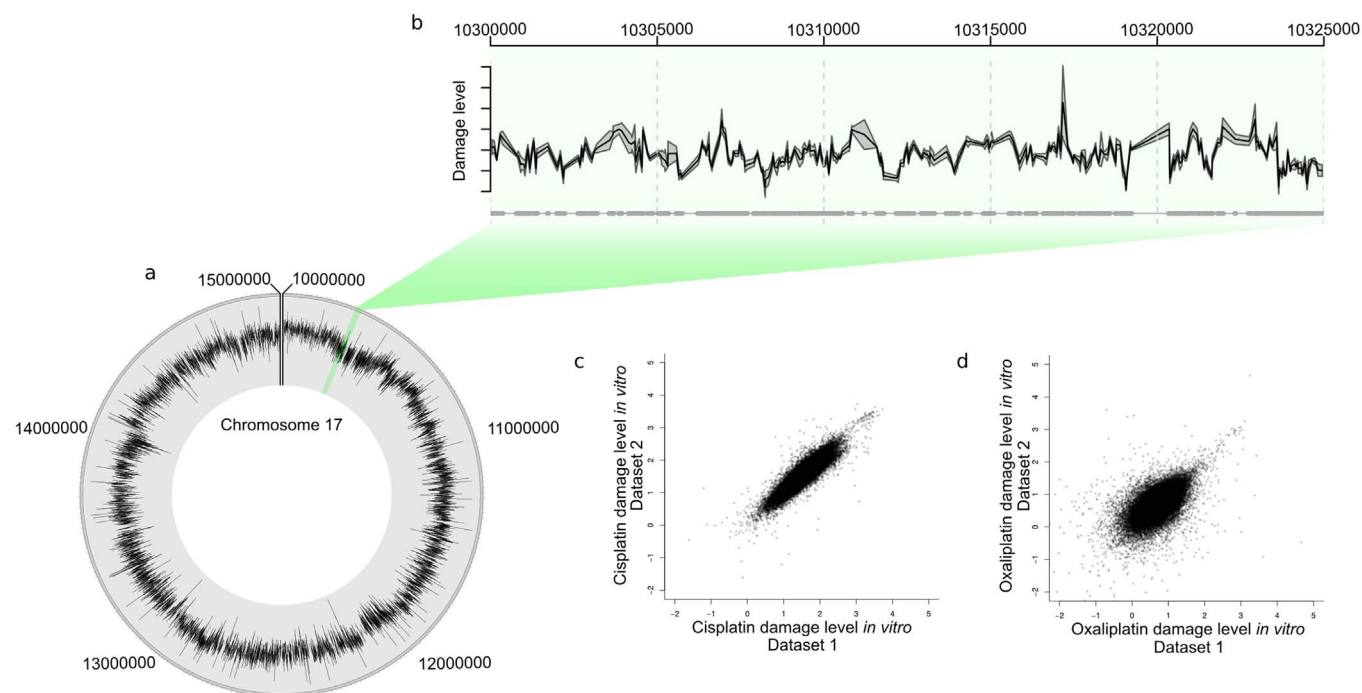| Treatment		Human correlations between:		Yeast correlations between:	
		3D-DIP-Chip and prediction	3D-DIP-Chip replicates	3D-DIP-Chip and prediction	3D-DIP-Chip replicates
Cisplatin	*In vivo*	0.61	0.82	0.54	0.54
	In vitro	0.67	0.92	0.56	0.72
Oxaliplatin	*In vivo*	0.40	0.74	0.53	0.55
	In vitro	0.41	0.59	0.51	0.55
UV	*In vivo*	0.51	0.77	-	-
	In vitro	0.56	0.85	-	-

Figure 2 | Human *in vitro* platinum induced DNA damage. (a) Circos plot of the whole dataset demonstrating the heterogeneity of the damage pattern. (b). 25Kbp section of data (produced in Sandcastle), showing the mean (black line) and standard error (grey shading) of two datasets and probe positions (grey dots). (c) and (d) Scatter plots showing the relationship between cisplatin and oxaliplatin repeat datasets respectively (plot (d) has been scaled to the same axis limits as plot (c), resulting in a small number of probes not being shown).

are common to different DNA damaging agents and could provide insight into how these events are organised in the epigenome.

Discussion

We have developed a method for measuring genomic DNA damage on microarrays. We first introduced the concept to measure CPD induction in *S. cerevisiae* following exposure to UV irradiation[13]. In the current report we have extensively modified, adapted and, most importantly, validated, this 3D-DIP-chip assay for use in both human and yeast cells to measure different types of DNA damage with sensitivity and at a high resolution over the entire yeast genome and a 10 Mbp section of the human genome. This represents a significant technological advance in the measurement of genetic damage at a high resolution on a genomic scale. The key methodological modifications made to the original 3D-DIP-chip assay, which allowed successful measurement of DNA damage in human cells can be summarised by developments in two key areas. Firstly, the DIP protocol was optimised by improving the immunoaffinity capture stage. This involved increasing the stringency of the post IP washes, and using a phenol-chloroform based post-DIP purification method. Secondly, an alternative method was used for amplifying the DIP sample prior to microarray hybridisation using a proprietary whole genome amplification method (WGA2, Sigma-Aldrich) instead of ligation-mediated PCR. This advance in the application of microarray-based technology now offers a novel method and protocol for examining DNA damage in human and other cells. The detailed methods that we describe here provide the basis for the analysis of many other types of DNA damage to which antibodies have been, or could be produced, opening the way to the genome-wide analysis of the full spectrum of genetic lesions.

The method is a significant advance compared to existing technologies, and represents an important new application of microarrays. Current technologies can measure DNA damage at high-resolution in single genetic loci at individual nucleotide resolution. These include the use of sequencing gels[18]. In addition, low-resolution methods such as immuno-slot-blot assays of total genomic DNA samples are also used[19]. The high-resolution techniques cover only very small sections of a genome and the low-resolution techniques do not offer sufficient sensitivity to be of use in many industrial applications, particularly in clinical and genotoxicity testing scenarios. It is worth noting that next generation sequencing technologies may in the future offer an alternative to the use of microarrays following the 3D-DIP stage of the protocol and we are indeed currently examining this. Others have already established
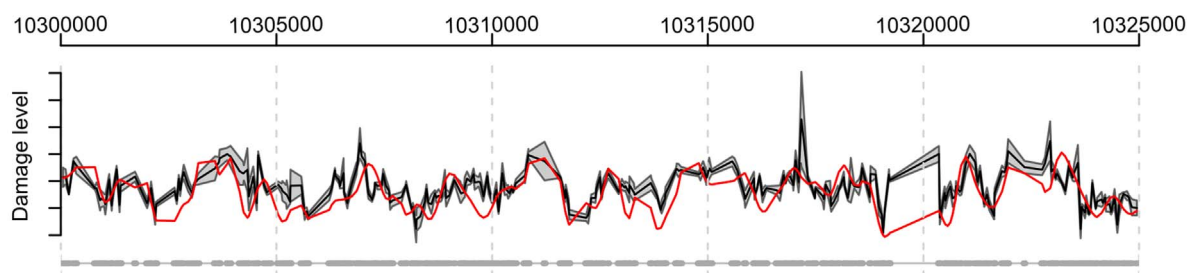

Figure 3 | Validating the 3D-DIP-Chip data. Section of human chromosome 17 showing mean (black line) and standard error (grey shading) of two cisplatin induced DNA damage datasets along with the predicted profile (red line) based on the genome sequence.
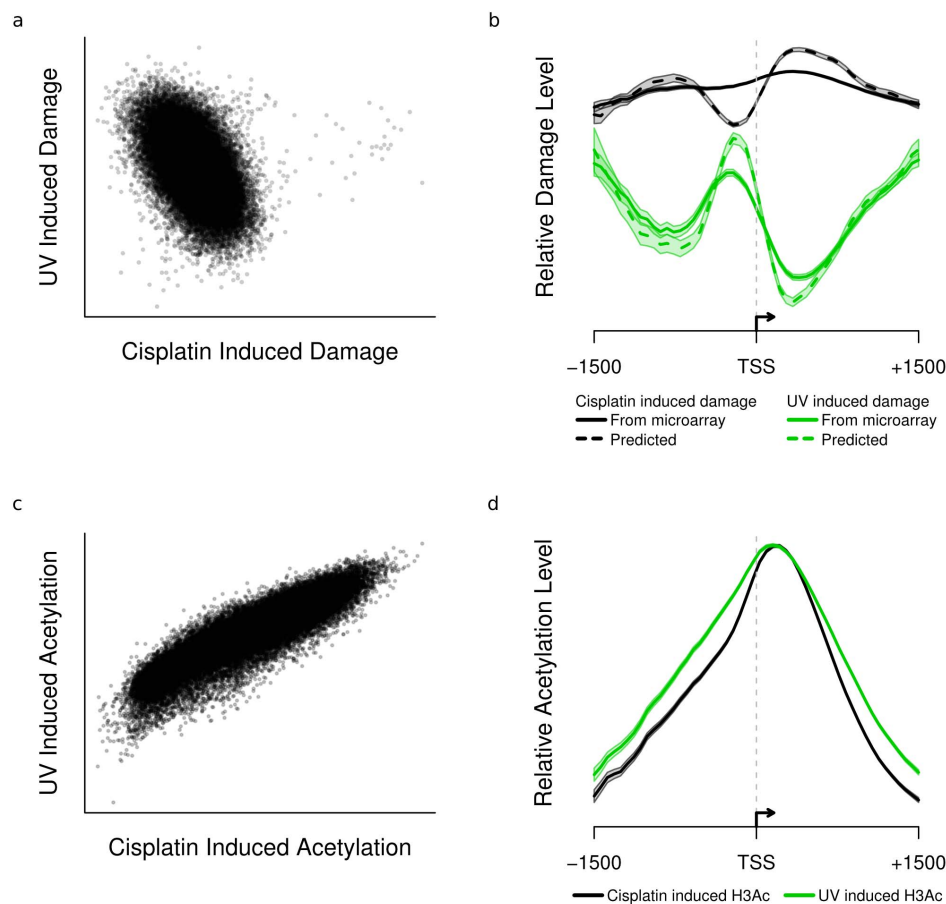
Figure 4 | Examples of the types of analyses that may be undertaken with 3D-DIP-Chip and ChIP-chip. Scatter plots show an inverse association between cisplatin and UV induced DNA damage (a) but a positive association between cisplatin and UV induced histone acetylation (c). Plotting the data around transcription start sites (TSSs) shows different patterns of damage induction with the two damaging agents (b; UV solid green line, cisplatin solid black line) along with similar predicted patterns (UV dashed green line, cisplatin dashed black line). Standard errors for all TSSs are shown as a shaded region. Histone acetylation around the same TSSs shows similar patterns with both damaging agents (d; same colouring as b).

techniques for measuring double strand breaks using next generation sequencing[20], using a technique that identifies the location of the DNA double strand breaks. We have developed a high-resolution technology, which can measure and locate DNA damage induction across a whole genome simultaneously. This now offers a functional assay capable of examining the DNA damaging lesions directly with significant relevance in the fields of genotoxicity testing, translational and personalised medicine, as well as in basic mechanistic laboratory studies investigating DNA damage and repair. For example, we are now using this method to examine clinical samples to characterise genomic DNA damage signatures that could be used as predictive biomarkers of response to the effects of DNA damaging chemotherapeutic agents, which may subsequently allow personalised therapy.

Using platinum-induced DNA damage and UV-induced CPD formation as a paradigm for DNA damage, we validate DIP in capturing damaged DNA fragments with highly reproducible qRT-PCR data. We confirm this by comparing our experimental data with the predicted DNA damage patterns derived from algorithms developed following the use of other techniques for measuring damage in naked DNA. Furthermore, we report the detailed protocols for the measurement of two important sources of DNA damage; environmental UV radiation and cisplatin and oxaliplatin used extensively in chemotherapy treatment regimens for patients with solid tumours. The ability to examine platinum-induced DNA damage and its repair using these methods will offer important mechanistic and clinical information relating to the use of these drugs, particularly with regard to drug resistance for this therapy. As described, our approach

allows us to map DNA damage events across whole genomes and to detect regions of preferential damage induction and repair within the genome, offering insight into the mechanisms of drug resistance. The data we show in Figure 4 for example demonstrates the power of these analyses by highlighting the genome-wide relationships for both the damage induced histone H3 acetylation pattern and UV versus cisplatin induced damage patterns respectively (Figure 4 a and b). More importantly, however, are the subtle differences that can be discerned by plotting the data in relation to genomic locations such as transcription start sites as shown in Figure 4 b and d. Examining the data in this way enables differences in genetic and epigenetic changes to be detected according to their genomic location. These deviations from the predicted pattern are unlikely to be caused by repair of DNA damage in these regions in this case, since the data is derived from the DNA of cells, which was extracted immediately after DNA damage treatment. A possible explanation for the departure from the predicted pattern is that the *in vivo* induced damage pattern may be affected by differences in the epigenome and chromatin structure at specific genomic locations, which is not accounted for by the predicted pattern, since these are determined from data derived from DNA damage frequencies measured in naked DNA. Understanding DNA damage in the context of chromatin is fundamental for determining the impact of the chromatin structure on the extent and pattern of genome-wide DNA damage. How chromatin structure influences DNA damage induction throughout whole genomes and how epigenetic responses relate to the genomic damage induction remains to be determined. We present histone

H3K14 acetylation data in response to UV and platinum exposure as a paradigm for how this can be achieved. We confirm histone H3K14 acetylation to be a prominent histone modification taking place globally in the genome following exposure to two different DNA damaging agents and that this response is remarkably consistent in the case of these two types of DNA damage. These results demonstrate the significant advantages of our method to understanding the effects of DNA damage on the epigenome at the genomic scale.

Furthermore, this technology can be considered as a paradigm for examining other DNA damages, providing that specific antibodies against that damage, or some other means of affinity capturing the damage, are available. As mentioned, this technology also has implications in the field of genotoxicity testing, where assessments of the efficacy and toxicity of new compounds are often still made based on simple laboratory assays or animal models. Our assay could be helpful in defining targets of new chemotherapeutic agents, delineating target sequences for DNA damage and detecting the unintended genomic damage, the so-called off-targets, caused by new pharmacology agents, such as those targeting the epigenome. Finally, next generation sequencing technologies are offering remarkable insight into the acquisition of mutations in genomes including cancer genomes. The results of these analyses appear to reveal the life history of mutagen exposure and, in addition, clearly reflect the associated DNA repair capacity of the cells in question. The 3D-DIP-chip assay described here could be used to further refine our understanding of the mechanisms of mutation, offering the possibility of identifying predictive DNA damage and repair signatures associated with subsequent mutational end-points and tumourigenesis.

Methods

Platinum analogue chemotherapy drugs. Cisplatin and oxaliplatin were obtained courtesy of the pharmacy department of Velindre Cancer Centre, Cardiff. The clinical formulations, at a concentration of 3.3 mM for cisplatin and 12.6 mM for oxaliplatin, were stored at 4°C. 2.5 mM cisplatin and 2.5 mM oxaliplatin treatments were used for both the DNA *in vitro* and *in vivo* human and yeast cell treatments for the microarray studies.

Yeast strains, culture and storage. The haploid, wild-type, *S. cerevisiae* strain used in these studies was BY4742 (MATα his3Δ1 leu2Δ0 lys2Δ0 ura3Δ0). Glassware and Yeast Extract Peptone Dextrose (YPD) media was sterilised by autoclaving at 121°C for 15 minutes, and all manipulations were undertaken in standard sterile conditions. All incubations were conducted at 30°C at 180 rpm in an Infors HT multitron standard incubator, unless otherwise stated. BY4742 cells were stored and grown in YPD media. For long-term storage, cells were grown to logarithmic-phase in YPD, glycerol was added to a final concentration of 30%, and cells were frozen at −80°C. Pre-cultures were grown by inoculating cells in 10 ml of YPD, incubating until cells reached stationary phase and storing these at 4°C. Pre-calculated amounts of pre-culture were then used to inoculate large volumes of YPD media as required for each experiment. For all experiments, cultures were incubated overnight to a density of 2×10^7 cells/ml. Cell density was calculated using a Neubauer cell counting chamber (Hawksley).

In vivo platinum treatment of yeast cells. Wild-type yeast BY4742 cells were grown to logarithmic-phase in YPD and collected by centrifugation at 5000 rpm for 5 minutes and resuspended in chilled phosphate-buffered saline (PBS) at a concentration of 2×10^7 cells/ml. 250 ml of resuspended cells were incubated with the required concentration of cisplatin or oxaliplatin (as mentioned above) in PBS for 4 hours, and untreated cells were incubated in PBS alone. Following incubation, cells were immediately collected by centrifugation at 5000 rpm for 5 minutes at room temperature and washed twice with chilled PBS ready for DNA preparation. For DNA damage studies, DNA was extracted immediately following treatment of cells and for histone H3 acetylation studies with chromatin, following treatment in PBS and collection, cells were resuspended in YPD and placed in the incubator for 60 minutes.

Preparation of yeast DNA. Both untreated and platinum treated cells were resuspended in 5 ml of sorbitol-Tris- ethylenediamine tetra acetate (sorbitol-TE) solution and mixed well. 0.5 ml of zymolyase 20 T (10 mg/ml in sorbitol solution) and 0.5 ml of 0.28 M β- mercaptoethanol were added and samples mixed by shaking. Cells were incubated overnight at 4°C. Spheroplasts were collected by gentle centrifugation at 2000 rpm for 5 minutes at 4°C and resuspended in 5 ml of lysis buffer/PBS 1 : 1(v/v) solution (DNA lysis buffer 4 M urea, 200 mM NaCl, 100 mM Tris-HCl [pH 8.0], 10 mM CDTA, 0.5% SDS). 500 μl of 10 mg/ml RNase A was added and samples were vortexed and incubated at 37°C for 1 hour. Following incubation, 200 μl of proteinase K (10 mg/ml in TE buffer) solution was added and samples were incubated for 2 hours at 65°C with occasional shaking. Two phenol/

chloroform (6 ml) DNA extractions and one chloroform (6 ml) DNA extraction were carried out to ensure complete deproteinisation. Equal volumes of phenol/chloroform were added (1 : 1 v/v), and samples shaken vigorously followed by centrifugation at 10,000 rpm (Beckman-Coulter centrifuge, JA-20 rotor) for 10 minutes and transfer of the upper aqueous phase to 15 ml Falcon tubes. DNA was recovered by precipitation using two volumes (12 ml) of pre-chilled 100% ethanol and storing at −20°C overnight. DNA pellets were collected by centrifugation at 4000 rpm for 15 minutes at 4°C and resuspended in 1 ml of TE buffer. After being completely dissolved, the DNA was reprecipitated by adding 1 ml of pre-chilled 100% isopropanol, with gentle shaking. DNA precipitate was removed by pipette tip, resuspended in 1 ml of TE buffer and DNA checked for purity and amount by non-denaturing agarose gel electrophoresis and UV spectrophotometry (NanoDrop-1000, NanoDrop Technologies, Thermo Scientific).

In vitro platinum treatment of yeast DNA. For *in vitro* platinum treatment, extracted naked genomic yeast DNA in TE was incubated with cisplatin or oxaliplatin, added from stock solution giving the required final drug concentration. DNA was incubated with cisplatin or oxaliplatin for 2 hours at 37°C and DNA recovered by ethanol precipitation. Precipitation was conducted by adding 2.5 × volume 100% ethanol, incubating at -80°C for 20 minutes, then at −20°C for 30 minutes, followed by centrifugation at 13500 rpm (Beckman-Coulter Microfuge 22R) for 20 minutes at 4°C. DNA pellets were washed with 75% ethanol and centrifuged a second time at 13500 rpm for 20 minutes at 4°C. Pellets were dried using a SpeedVac system (Thermo Savant) and resuspended in 100 μl TE prior to sonication and DIP.

Preparation of yeast chromatin. Wild-type yeast BY4742 cells were grown to logarithmic-phase in YPD and treated *in vivo* as described above. Cells were treated with 250 μM cisplatin or oxaliplatin for four hours and following treatment resuspended in YPD for the required repair time. Cells were crosslinked using 3 ml of 37% formaldehyde, per 100 ml culture, for 10 minutes at room temperature on a shaking platform. Crosslinking was quenched using 5.5 ml of 2.5 M glycine for 5 minutes at room temperature on a shaking platform. Cells were collected by centrifugation at 5000 rpm for 5 minutes at 4°C (Beckman- Coulter centrifuge, JA-10 rotor), and washed twice by resuspending in 40 ml of ice cold PBS and collecting by centrifugation as before. Cells were resuspended in 1 ml FA/SDS (+PMSF) and transferred to a 2 ml microcentrifuge tube. Cells were collected by centrifugation at 13500 rpm for 5 minutes at 4°C (Beckman-Coulter Microfuge 22R), the supernatant was removed and the pellet was resuspended again in 0.5 ml FA/SDS (+PMSF) in a 2 ml microcentrifuge tube. Cells were mechanically lysed by adding 500 μl of glass beads to each sample and vortexing for 10 minutes at 4°C. The cell lysate was retrieved by puncturing a hole in the 2 ml microcentrifuge tube with a hot needle and placing it in a 15 ml Falcon tube and centrifuging briefly at 2000 rpm for 2 minutes at 4°C (Eppendorf centrifuge 5810R). The glass beads were washed with 500 μl of FA/SDS (+PMSF) and centrifuged again at 2000 rpm for 2 minutes at 4°C. Cell lysate was transferred to a 2 ml microcentrifuge tube and centrifuged at 4000 rpm for 20 minutes at 4°C (Beckman-Coulter Microfuge 22R) to remove any soluble, non-crosslinked proteins. The supernatant was removed and the pellet was resuspended in 1 ml FA/SDS (+PMSF) and sonicated using a BioRuptor sonicator (Diagenode) with power set at the 'high' position for 8 cycles of 30 seconds on and 30 seconds off at 4°C. Following sonication a further centrifugation was performed at 13000 rpm for 10 minutes at 4°C and the supernatant was collected and centrifuged again at 13000 rpm for 20 minutes at 4°C (both using Beckman-Coulter Microfuge 22R). The supernatant containing the chromatin was snap frozen in liquid nitrogen and stored at −80°C.

Human cell lines. AG16409 (normal human dermal fibroblast) cells were obtained from the Coriell Cell Repository (Camden, NJ, USA). AG16409 cells were transduced with an amphotropic retrovirus expressing the catalytic subunit of telomerase, human telomerase reverse transcriptase (hTERT). Telomerase activity was confirmed by the telomeric repeat amplification protocol (TRAP) assay, ensuring immortalisation of fibroblasts (AG16409) tert.

Human cell culture. All manipulations were undertaken in standard sterile conditions and all glassware was sterilised by autoclaving at 121°C for 15 minutes. Fibroblasts were grown as monolayers at 37°C in a humidified incubator, under an atmosphere containing 5% CO_2. Fibroblast growth media comprised Dulbecco's Modified Eagle Medium (DMEM: Gibco by Life Technologies, Invitrogen, Paisley, UK), supplemented with 10% fetal calf serum, 1% L-Glutamine and 1% penicillin-streptomycin (all Sigma- Aldrich, Dorset, UK). Fibroblasts were cultured in 10 ml of growth media in T75cm 2 cell culture flasks or in 5 ml of media in T25cm 2 cell culture flasks and replenished with fresh growth medium approximately every 3 days. Cells were reseeded and maintained in new cell culture flasks approximately every 4 weeks and were seeded and cultured on tissue culture dishes for drug treatments. Fibroblasts were routinely passaged close to confluence (~80–90% confluent) every 7-10 days, when cells were trypsinised and $\sim 2 \times 10^5 – 4 \times 10^5$ cells were reseeded. Briefly, cells were trypsinised by removing growth media from the flask followed by washing with 2 ml of warmed PBS to remove residual media and serum. 2 ml of 1 X trypsin-EDTA (Gibco by Life Technologies, Invitrogen) was added and fibroblasts were returned to the incubator at 37°C for 15–30 minutes. When cells had detached from the surface of the flask they were resuspended in the required amount of growth media for reseeding. Cells were counted using an improved Neubauer haemocytometer (Hawksley) and 10 μl of cell suspension was pipetted under the

coverslip of the haemocytometer. For these cells the PD was ~0.4 PD/day and this remained constant throughout these experiments.

Preparation of human DNA and *in vivo* platinum treatment and UV irradiation. Approximately 2×10^5–4×10^5 cells were seeded on to tissue culture dishes (100 × 20 mm), yielding approximately 2×10^6 cells following growth for 7–10 days. Alternatively, larger tissue culture dishes (150 × 25 mm) would yield 4–5×10^6 cells after 10 days incubation. Cells were grown to confluence before treatment in each case.

Stock solutions of cisplatin and oxaliplatin were diluted to the required concentration using serum-free media. Growth media was removed from cells in tissue culture dishes, cells were washed twice with 2 ml of warmed PBS (5 ml PBS used for the larger tissue culture dishes), and serum-free media containing the platinum analogue at the required concentration was added. Dishes were returned to the incubator for 2 hours at 37°C. Untreated cells were also incubated for 2 hours in serum-free media. Following incubation, cells were harvested with 1 x trypsin-EDTA. PBS was added to the cell suspension and this was transferred to a 15 ml Falcon tube and centrifuged at 1000 rpm for 5 minutes at room temperature (Eppendorf centrifuge 5810R). The supernatant was removed from the cell pellet and the cells processed directly for DNA extraction using the Qiagen DNeasy Blood & Tissue Kit (Qiagen No. 69504).

For UV treatment, growth media was removed and cells were washed twice with 2 ml of warmed PBS. 5 ml of PBS was then added to the tissue culture dish for UV treatment, and untreated cells were also placed in 5 ml of PBS. Cells were irradiated with 254 nm UVC irradiation from a calibrated germicidal VL-21G mineralight lamp (UV products, San Gabriel, CA, USA) at a fluence of 10 J/m²/s for 5 seconds, giving a total dose of 50 J/m². Following treatment cells were immediately harvested using trypsin and genomic DNA was extracted using the Qiagen DNeasy Blood & Tissue Kit.

Human DNA treated *in vitro* with platinum and UV irradiation. Cisplatin or oxaliplatin was added from stock solution to genomic DNA (suspended in buffer AE, the elution buffer solution of the Qiagen DNeasy Blood & Tissue Kit), to give the required final drug concentration. DNA was incubated with cisplatin or oxaliplatin for 2 hours at 37°C and recovered by ethanol precipitation. Precipitation was conducted by adding 2.5 × volume 100% ethanol, incubating at −80°C for 20 minutes, then at −20°C for 30 minutes, followed by centrifugation at 13500 rpm for 20 minutes at 4°C (Beckman-Coulter Microfuge 22R). DNA pellets were washed with 75% ethanol and centrifuged a second time, at 13,500 rpm for 20 minutes at 4°C. Pellets were dried using the SpeedVac system (Thermo Savant) and resuspended in 100–200 μl of the buffer AE elution buffer prior to sonication and DIP.

For UV treatment genomic DNA, in buffer AE, was transferred to 35 × 10 mm tissue culture dishes and irradiated as described in previous section with UV at a dose of 300 J/m². Following treatment, DNA was returned to microcentrifuge tubes (Eppendorf) for fragmentation with sonication followed by DIP.

DNA and chromatin fragmentation by sonication. DNA and chromatin were fragmented using a BioRuptor sonicator (Diagenode). Four 1.5 ml microcentrifuge tubes, each containing 200 μl of DNA or chromatin sample, were placed in a 1.5 ml microtube unit, and the unit placed in a cooling water bath. For human DNA each sample was diluted to 100 ng/μl prior to sonication to ensure reproducibility. Power was set at the 'high' position and sonication was conducted at 4°C. The number of cycles of sonication employed was different between samples, firstly because chromatin fragments more readily than naked DNA and therefore fewer cycles are required. Secondly, for human samples a shorter fragment length was required to improve microarray resolution. For yeast studies, a fragment length of 300–500 bp was used, whilst for human studies a shorter fragment length of 200–300 bp was required. Sonication schedules employed were as follows:-

Yeast DNA - 20 cycles of 30 seconds on, 30 seconds off
Yeast chromatin - 8 cycles of 30 s on, 30 s off
Human DNA - 25 cycles of 30 s on, 30 s off

Satisfactory sonication was confirmed by gel electrophoresis using a 1.2% agarose gel and using the FastRuler™ low range DNA ladder (Fermentas) for reference.

Quantitative real-time PCR (Q-PCR). Quantitative real-time PCR was performed using the iQ™ SYBRgreen supermix (Bio-Rad) and the iCycler MyiQ™ real-time PCR detection system (Bio-Rad). For yeast studies primers for the promoter of the *MFA2* gene were used and for human studies primers for the human 28S ribosomal RNA gene were used. For yeast studies the qRT-PCR reaction was performed using the following PCR program: 1. 95°C for 3 minutes, 2. 95°C for 15 seconds, 3. 55°C for 20 seconds -followed by plate reading. Steps 2–3 were repeated 44 times. In addition a melt curve was undertaken to ensure a single PCR product and all samples were amplified in triplicate. For human studies the qRT-PCR reaction was performed using the following PCR program: 1. 95°C for 3 minutes, 2. 95°C for 10 seconds, 3. 60°C for 20 seconds - followed by plate reading. Steps 2–3 were repeated 44 times.

The *MFA2* promoter primer sequences:-
Forward: 5′ - AAAGCAGCATGTTTTCATTTGAAACA - 3′
Reverse: 5′ - TATGGGCGTCCTATGCATGCAC - 3′

The 28S rRNA primer sequences:-
Forward: 5′ - CGCAATACGAATGCCCCCG - 3′
Reverse: 5′ - AGCCGCCTGGATACCGC - 3′

DNA immunoprecipitation damage of platinum-induced DNA damage. Fragmented yeast or human DNA treated *in vivo* or *in vitro* with platinum analogues, as described, was used for DIP using the anti-cisplatin modified DNA, CP9/19, antibody (ab103261, Abcam). 40 μl of Dynabeads (Sheep anti-Rat IgG, Invitrogen) per sample were washed three times using 500 μl PBS-BSA (0.1% of BSA). Washed Dynabeads were resuspended in 50 μl of PBS-BSA (0.1% of BSA) per sample and 0.5 μg of CP9/19 antibody was added per 40 μl of Dynabeads for the detection of cisplatin-induced DNA damage or 1.5 μg of antibody added per 40 μl of Dynabeads for the detection of oxaliplatin-induced damage. Dynabeads and antibody were incubated at 30°C for 30 minutes at 1300 rpm in a thermomixer (Eppendorf). Dynabeads were collected, washed three times with 500 μl of chilled PBS-BSA (0.1% of BSA) and resuspended in 50 μl of PBS-BSA (0.1% of BSA) per sample. 30 μl of 10 X PBS-BSA (1% of BSA) and 6 μg of sonicated DNA were added to each tube containing the Dynabeads, and the final volume made up to 300 μl with PBS. Samples were incubated at 21°C for 3 hours at 1300 rpm in a thermomixer. Following incubation, samples underwent a series of washes as follows: first wash with 500 μl of freshly prepared FA/SDS buffer. This was followed by three washes with 500 μl of FA/SDS containing 0.5 M NaCl (for yeast samples) or 1 M NaCl (for human samples), one wash with 500 μl of LiCl solution and one wash with 500 μl of cold TE. DNA was eluted from the Dynabeads in 125 μl of 1 x pronase buffer at 65°C at 900 rpm for 30 min in a thermomixer (Eppendorf). 6.25 μl of pronase (20 mg/ml) was added and samples incubated in a water bath at 65°C overnight. IN samples of 0.6 μg (1/10 of IP sample) of sonicated DNA were made up to 100 μl with TE buffer followed by the addition of 25 μl of 5 x pronase buffer and 6.25 μl of pronase (20 mg/ml) and incubated in a water bath at 65°C overnight. Following overnight incubation, IP and IN samples were processed for removal of the DNA damage (see next section), and 5 μl of DNase-free RNase A (10 mg/ml) was added during this process. DNA was then purified and for yeast samples this was achieved using the PureLink™ Quick PCR Purification Kit (Invitrogen) and eluted in 50 μl of elution buffer and for human DNA samples it was achieved using a phenol-chloroform extraction method. Finally, to increase the overall DNA yield in the human DIP samples, DIP samples were processed in parallel and two samples pooled prior to the qRT-PCR stage.

Removal of platinum adducts prior to qRT-PCR and microarray preparation. DIP DNA fragments detected by the CP9/19 antibody and the corresponding IN DNA samples will contain platinum adducts (apart from untreated samples), which are known to inhibit DNA polymerase function and interfere with microarray hybridisation. These samples therefore require processing for removal of these adducts prior to downstream applications. Platinum-DNA adducts are very stable over a long period of time, but in the presence of cyanide ions most platinum residues are known to be removed from DNA[10]. Sodium cyanide (NaCN) has been proven to be the most effective chemical for disrupting platinum-DNA adducts[10–12] and in the DIP studies described in this paper, NaCN was used to remove platinum adducts. Following overnight incubation of the IP and IN samples with pronase DNA samples were incubated with 0.2 M NaCN for 2 hours at 65°C. 5 μl of RNase A (10 mg/ml) was added for the last 45 minutes of this incubation. Following incubation, DNA samples were purified as described in the previous section.

Removal of CPDs prior to qRT-PCR and microarray preparation. Similar to work examining the platinum adducts, CPDs also needed removal prior to qRT-PCR, WGA and microarray hybridisation and this was achieved using the proprietary PreCR DNA repair kit (New England Biolabs) - a kit that removes many DNA damages including CPDs. 40 μl of IP and IN samples were processed for repair using this kit as per the manufacturer's instructions. Following repair, DNA was purified using phenol-chloroform extraction and ethanol precipitation and resuspended in 10 μl.

Chromatin immunoprecipitation of histone H3K14 acetylation. Yeast chromatin extracted from cells treated *in vivo* with platinum analogues was used for chromatin immunoprecipitation (ChIP) using the anti-acetyl-histone H3(lysine14) antibody (Millipore, 07-353). 50 μl of Dynabeads (Sheep anti-Rabbit IgG, Invitrogen) per sample were washed three times using 500 μl PBS-BSA (0.1%). Washed Dynabeads were resuspended in 50 μl of PBS-BSA (0.1%) per sample and 2 μl of anti-acetyl-histone H3 (lysine14) antibody was added per 50 μl of Dynabeads for detection of histone H3 K14 acetylation. Dynabeads and antibody were incubated at 30°C for 30 minutes at 1300 rpm in a thermomixer (Eppendorf). Dynabeads were collected, washed three times with 500 μl of chilled PBS-BSA (0.1%) and resuspended in 50 μl of PBS-BSA (0.1%) per sample. 30 μl of 10 X PBS-BSA (10 mg/ml) and 125 μl of sonicated chromatin were added to each sample containing the Dynabeads, and the final volume made up to 300 μl with PBS. Samples were incubated at 21°C for 3 hours at 1300 rpm in a thermomixer. Following incubation, samples underwent a series of washes as follows: first wash with 500 μl of freshly prepared FA/SDS buffer. This was followed by three washes with 500 μl of FA/SDS + 500 mM NaCl, one wash with 500 μl of LiCl solution and one wash with 500 μl of cold TE. Chromatin was eluted from the Dynabeads in 125 μl of pronase buffer at 65°C at 900 rpm for 30 min. 6.25 μl of pronase (20 mg/ml) was added to each sample and incubated at 65°C in a water bath overnight. IN samples of 25 μl of sonicated chromatin were made up to 100 μl with TE buffer followed by the addition of 25 μl of 5 x pronase buffer and

6.25 µl of pronase (20 mg/ml) and incubated overnight as the IP samples. Following overnight incubation, IP and IN samples were processed for damage removal with sodium cyanide as discussed previously, and 5 µl of DNase- free RNase A (10 mg/ml) was added during this process. DNA was purified using the PureLink TM Quick PCR Purification Kit (Invitrogen) and eluted with 50 µl elution buffer.

Sample Preparation for yeast DNA microarray hybridisation. Yeast DIP and ChIP and input samples were processed for microarray hybridisation as described in the Agilent Technologies Yeast ChIP on chip protocol (Agilent Technologies Yeast ChIP-on-chip Analysis Protocol, version 9.2), and as outlined previously[14]. Briefly, the steps required are blunting of the ends of the DNA fragments followed by ligation of a common linker sequence of DNA to the ends of these fragments, ligation-mediated PCR amplification (LM-PCR), labelling and hybridisation to 4 × 44k format Agilent yeast microarrays. Following amplification the concentration of DNA was measured with the NanoDrop spectrophotometer and sample concentration was normalised to 150 ng/µl with H$_2$O. 10.5 µl of the IP and IN samples were differentially fluorescently labelled with Cy5 and Cy3 fluorophores respectively using the BioPrime Total Genomic Labelling System (Invitrogen), which yields sufficient quantities of labelled DNA for hybridisation to microarrays. For labelling, samples were incubated for 2 hours at 37°C. Labelling efficiency was determined using the MicroArray Measurement Module on the NanoDrop ND-1000 Spectrophotometer, which measures DNA concentration and labelling effectiveness. Following labelling, the IP and IN samples were combined and 110 µl of the hybridisation mixture applied to each Agilent yeast 4 × 44k microarray. Mixtures were allowed to hybridise to microarrays for 24 hours at 65°C. The 4 × 44k microarray format signifies that 44,000 features are imprinted on a single microarray to represent the entire yeast genome and that 4 microarrays are printed on each glass slide. The method for each of the preparatory microarray steps of DNA end-blunting, linker ligation, PCR amplification, labelling and hybridisation were all conducted as described previously[14].

Sample Preparation for human DNA microarray hybridisation. Human samples were prepared for microarray hybridisation differently to yeast samples. A proprietary whole genome amplification method GenomPlex Complete Whole Genome Amplification Kit (WGA2, Sigma-Aldrich) was used for amplification rather than LM-PCR. This removed the need for a second round of PCR amplification preventing the introduction of amplification bias. This kit uses an amplification method based on conversion of genomic DNA fragments into PCR-amplifiable OmniPlex library molecules flanked by universal priming sites. The OmniPlex library is then PCR amplified using universal oligonucleotide primers to generate a representative amplification of human genomic DNA.

The manufacturer's protocol was followed except that the initial fragmentation step was eliminated since our samples were already fragmented. The entire DIP sample was used for library preparation and 2 µl of 1 x library preparation buffer and 1 µl of library stabilization solution were added to the DIP sample, followed by mixing and incubating at 95°C for 2 minutes and immediately cooling on ice. 1 µl of library preparation enzyme was added to each sample, and samples incubated in a thermal cycler at 16°C for 20 minutes, 24°C for 20 minutes, 37°C for 20 minutes and 75°C for 5 minutes before proceeding to PCR amplification. 7.5 µl of 10 X amplification master mix, 47.5 µl of nuclease-free H$_2$O and 5 µl of WGA DNA polymerase were added to each sample, mixed and incubated in a thermal cycler as follows: 95°C for 3 minutes, followed by 14–16 cycles of 94°C for 15 sec and 65°C for 5 minutes. Samples were purified using the PureLink PCR Purification Kit (Invitrogen), eluted in 15 µl of water and DNA quantified using the MicroArray Measurement Module on the NanoDrop ND-1000 Spectrophotometer. The expected yield was between 1–5 µg of genomic material, providing enough material for one microarray experiment. Following amplification, samples were labelled as described before using the BioPrime Total Genomic Labelling System (Invitrogen) except that human samples were labelled for 3 hours at 37°C. Multiple labelled IP DNA samples could be combined prior to microarray hybridisation as a means to boosting the microarray signal and samples were hybridised as described above for 24 hours at 65°C to custom-designed Agilent Technologies human 4 × 44k microarrays.

Microarray washing, scanning and feature extraction. After hybridisation both the yeast and human microarrays were washed twice and scanned as described in the Agilent Technologies Yeast ChIP on chip protocol (Agilent Technologies Yeast ChIP-on-chip Analysis Protocol, version 9.2). The scanned image was analysed by Agilent Feature Extraction computer software, which converted the image into numerical values for data analysis. Microarray data analysis was conducted using the R statistical programming language (R version 2.15.2). All of the analysis presented in this paper was conducted using R using software developed in our laboratory.

1. Perkel, J. M. Life science technologies: animal-free toxicology: sometimes, in vitro is better. *Science* **335**, 1122 (2012).
2. Alexandrov, L. B. *et al.* Signatures of mutational processes in human cancer. *Nature* **500**, 415 (2013).
3. Yu, S., Teng, Y., Waters, R. & Reed, S. H. How chromatin is remodelled during DNA repair of UV-induced DNA damage in *Saccharomyces cerevisiae*. *PLOS Genet* **7**, e1002124 (2011).
4. Guo, R., Chen, J., Mitchell, D. L. & Johnson, D. G. GCN5 and E2F1 stimulate nucleotide excision repair by promoting H3K9 acetylation at sites of damage. *Nucleic Acids Res* **39**, 1390 (2011).
5. Saris, C. P., van de Vaart, P. J. M., Rietbroek, R. C. & Bloramaert, F. A. *In vitro* formation of DNA adducts by cisplatin, lobaplatin and oxaliplatin in calf thymus DNA in solution and in cultured human cells. *Carcinogenesis* **17**, 2763 (1996).
6. Woynarowski, J. M., Chapman, W. G., Napier, C., Herzig, M. C. S. & Juniewicz, P. Sequence-and region-specificity of oxaliplatin adducts in naked and cellular DNA. *Mol Pharmacol* **54**, 770 (1998).
7. Woynarowski, J. M. *et al.* Oxaliplatin-induced damage of cellular DNA. *Mol Pharmacol* **58**, 920 (2000).
8. Comess, K. M., Burstyn, J. N., Essigmann, J. M. & Lippard, S. J. Replication inhibition and translesion synthesis on templates containing site-specifically placed cis-diamminedichloroplatinum (II) DNA adducts. *Biochemistry* **31**, 3975 (1992).
9. Suo, Z., Lippard, S. J. & Johnson, K. A. Single d (GpG)/cis-diammineplatinum (II) adduct-induced inhibition of DNA polymerization. *Biochemistry* **38**, 715 (1999).
10. Lemaire, M. A., Schwartz, A., Rahmouni, A. R. & Leng, M. Interstrand cross-links are preferentially formed at the d(GC) sites in the reaction between cis-diamminedichloroplatinum (II) and DNA. *P Natl Acad Sci U S A* **88**, 1982 (1991).
11. Olinski, R., Briggs, R. C., Basinger, M. & Jones, M. M. Effectiveness of chemical agents in removing platinum from DNA isolated from cisplatin-treated HL-60 cells. *Acta Biochim Pol* **39**, 327 (1992).
12. Blommaert, F. A. & Saris, C. P. Detection of platinum-DNA adducts by 32P-postlabelling. *Nucleic Acids Res* **23**, 1300 (1995).
13. Teng, Y. *et al.* A novel method for the genome-wide high resolution analysis of DNA damage. *Nucleic Acids Res* **39**, e10 (2011).
14. Kartalou, M. & Essigmann, J. M. Recognition of cisplatin adducts by cellular proteins. *Mut Res-Fund Mol M* **478**, 1 (2001).
15. Fichtinger-Schepman, A. M. J., van Oosterom, A. T., Lohman, P. H. M. & Berends, F. Cis-diamminedichloroplatinum (ii)-induced DNA adducts in peripheral leukocytes from seven cancer patients: quantitative immunochemical detection of the adduct induction and removal after a single dose of cis-diamminedichloroplatinum (ii). *Cancer Res* **47**, 3000 (1987).
16. Mitchell, D. L., Jen, J. & Cleaver, J. E. Sequence specificity of cyclobutane pyrimidine dimers in DNA treated with solar (ultraviolet B) radiation. *Nucleic Acids Res* **20**, 225 (1992).
17. Tornaletti, S., Rozek, D. & Pfeifer, G. P. The distribution of UV photoproducts along the human p53 gene and its relation to mutations in skin cancer. *Oncogene* **8**, 2051 (1993).
18. Teng, Y., Li, S., Waters, R. & Reed, S. H. Excision repair at the level of the nucleotide in the *Saccharomyces cerevisiae* MFA2 gene: mapping of where enhanced repair in the transcribed strand begins or ends and identification of only a partial rad16 requisite for repairing upstream control sequences. *J Mol Biol* **267**, 324 (1997).
19. Perdiz, D. *et al.* Distribution and repair of bipyrimidine photoproducts in solar UV-irradiated mammalian cells possible role of dewar photoproducts in solar mutagenesis. *J Biol Chem* **275**, 26732 (2000).
20. Crosetto, N. *et al.* Nucleotide-resolution DNA double-strand break mapping by next-generation sequencing. *Nat Methods* **10**, 361 (2013).

Author contributions

J.R.P. conducted the majority of the experiments and assisted in writing the manuscript, M.B. analysed the data and developed the software to produce the figures, K.E.E. performed validation experiments using RT-PCR, S.Y. performed biological replicates, R.M.W. assisted with the development of the method, R.W. read the manuscript, N.S. read the manuscript and advised on method development, S.H.R. designed the experiments and wrote the manuscript.

Additional information

Supplementary information accompanies this paper at http://www.nature.com/scientificreports

Competing financial interests: The authors declare no competing financial interests.